

GROWTH OF ZNO NANOCRYSTALS IN ZNSE/ZNO:O ZNSE(0.5WT.%TE) NANOHETEROSTRUCTURES

NEMATOV SHERZOD QALANDAROVICH

Doctor of Physical and Mathematical Sciences, Professor Vice-rector for science and innovations

NISHONOVA NODIRAKHON RAIMJONOVNA

Professor, Doctor of Philosophy, Academician of the Turonian Academy of Sciences

ELMUROTOVA DILNOZA BAHTIYOROVNA

PhD in Physics and Mathematics PhD dosenet Tashkent State Technical University named after I.A. Karimov

Abstract

Represents the results on the formation of nanophase inclusions and the relationship of radiolysis with nonstoichiometry, as well as the role of lattice stresses in ZnO/ZnSe(Te):O nanoheterostructures. It is shown that the NHS ZnSe/ZnO:O had nanocrystalites up to 27 nm in size, and the NHS ZnSe(0.5wt.%Te)/ZnO up to 52 nm.

Keywords: Nanoheterostructure, nanocrystalites, zinc selenide, isovalent impurity, X-ray diffraction, X-ray fluorescence analysis.

Introduction

Semiconductor heterojunctions in nanostructures-quantum devices, used today in the world as optoelectronic materials with a tunable band width, have unusual electron transport and optical effects. The high intrinsic radiative efficiency of blue/green light-emitting diodes (p-n-injection) developed on the basis of ZnSe and ZnTe is due to the advantages of the nanoheterostructure configuration in the form of a quantum well and the fact that they are direct-gap semiconductors. A strong dependence of their optoelectronic characteristics on the sizes of nanoparticles is noted [1]. According to the X-ray diffraction analysis (XRD) spectra, it was shown that the addition of

nitrogen to ZnO led to an increase in the intensity of peaks 100, 002, 101, 102, 110, 103, 112, 201. ZnO NP 5 nm in size had orientations (100), (002), (101), (102), (110), (103), (112) [2]. X-ray diffraction analysis on the DRON-3 diffractometer (CuK α 1,2 radiation) showed high degree of orientation of ZnO nanorods with the (002) crystallographic axis along the normal to the substrate surface [3]. X-ray diffraction analysis of the n-ZnO/p-CuO HS showed that the n-ZnO film has hexagonal structure, on which the p-CuO monoclinic lattice is formed. X-ray diffraction analysis showed that polycrystalline thin-film n-ZnO/p-CuO HJs had (100), (002), (101), (102), (110), and (103) orientations [4]. It is also known from the literature that the Te isovalent impurity has a positive effect on the structural perfection of ZnSe crystals, which is associated with the completeness of the wurtzite–sphalerite phase transition. X-ray diffraction analysis showed that twins and stacking faults are found in ZnSe_{1-x}Te_x crystals at C_{Te}<0.3wt.%; C_{Te}≥0.6wt.% leads to tetragonal distortion of the crystal lattice [5]. Peaks (111), (220) (311) and (400) were observed in X-ray patterns of ZnSe in the region from 2 θ =10°–75° [6]. The self-ordering of Mg and O isoelectronic impurities in ZnSe is theoretically described, it is shown that the advantage in the formation of Mg-O and Zn-Se bonds over the formation of Mg-Se and Zn-O bonds leads to self-organization of Mg and O impurities in ZnSe in a wide concentration range [7].

However, detailed studies on the formation of possible nanophase inclusions, the relationship of radiolysis with nonstoichiometry, and the role of lattice stresses in ZnO/ZnSe(Te):O nanoheterostructures have not been carried out.

The aim of the study is to determine the crystal structure, size, shape and orientation of ZnO nanoparticles depending on the Zn/Se ratio and the Te impurity.

The object of study is ZnSe scintillator crystals subjected to tellurium implantation and heat treatment in an oxidizing environment [5].

Research methods: X-ray fluorescence analysis (XRF) was carried out on a multichannel analyzer with Ge detector in order to determine the total elemental composition averaged over the near-surface layer by selecting radioactive sources of x-ray excitation of k-lines of elements to the depth of the half-absorption layer of radiation. To determine the degree of nonstoichiometry of a crystal, i.e. the Se/Zn ratio in the near-surface layer is about 40 μ m, the ¹⁰⁹Cd isotope with an X-quanta energy of 22.1 keV was used, and the ²⁴¹Am isotope with an X-quantum energy of 59.6 keV was taken to find the Te impurity concentration in the 70 μ m layer, the error was no more than 0.1% [9, 12, 18].

X-ray diffraction analysis of the structure and phase composition (errors 1%); the structure and phase composition of the samples were studied by small-angle X-ray diffraction on DRON-3M diffractometer (radiation $\lambda_{\text{CuK}\alpha}=0.1542$ nm) in the angle range $2\theta=10\text{--}700$ [8-20]. An analysis of the obtained X-ray patterns makes it possible to determine the symmetry of the crystal structure, the crystallographic plane of the sample surface, and the general phase composition. X-ray beam collimation and the use of the small-angle scattering method make it possible to reveal both amorphous regions and crystalline inclusions and determine their sizes in the nanometer scale using the well-known Selyakov–Scherrer formula [10].

$$L = \frac{0.94\lambda}{\beta_{hkl} \cdot \cos \theta_{hkl}}$$

where L - the grain size (nm), λ - the wavelength of the radiation used, θ - the angle of reflection, β - the half-width of the corresponding reflection, in rad.

The error in determining the size of ZnO nanoparticles was no more than $\pm 1\%$.

Crystal structure and phase composition: The table shows the XPA data using an isotope source and a Si(Li) detector.

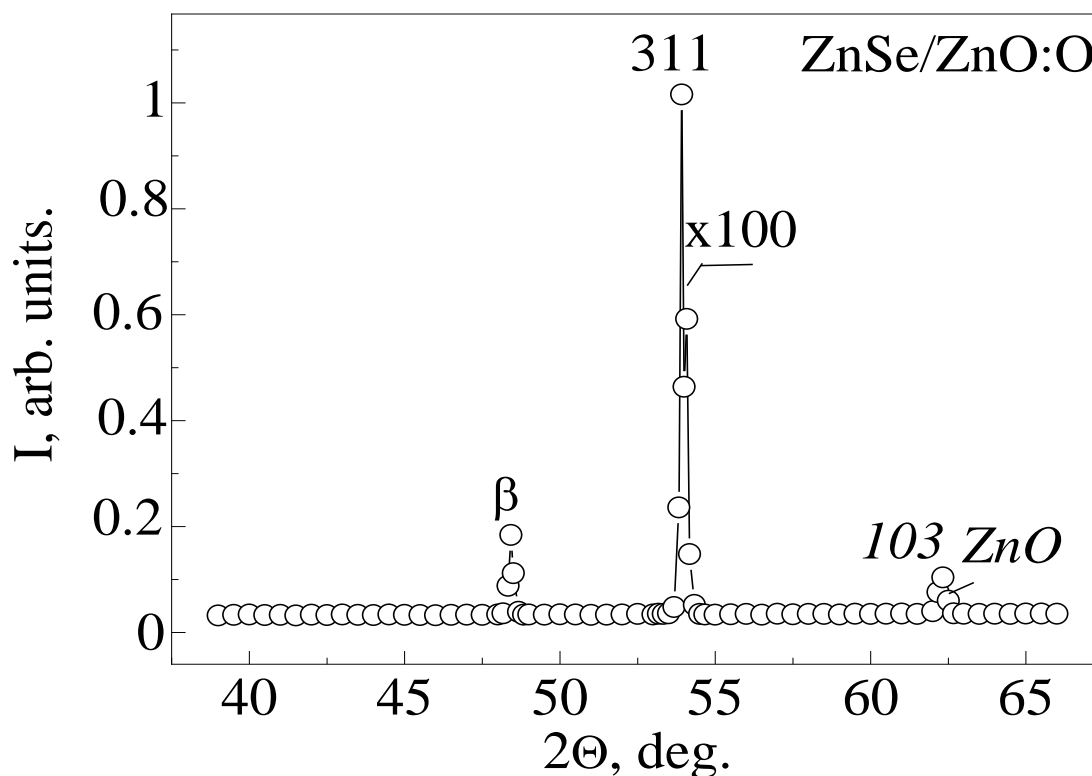
Table

Elemental composition of ZnSe single crystals

ZnSe:O and ZnSe(0.5%Te)			
Weight, gr	Conc. Zn, wt %	Conc. Se, wt %	Rel. Se/Zn
0.3586 - 0.3474	33.71 - 33.65	28.48 - 28.71	0.845 - 0.853

It can be seen from the table that the samples in the near-surface layer were nonstoichiometric and contained 1 wt % excess Zn. The super-stoichiometry of Zn, due to the volatility of Se, increases after doping with Te, due to the difference in the bond strengths of Zn-Te, Zn-Se, and Zn-O.

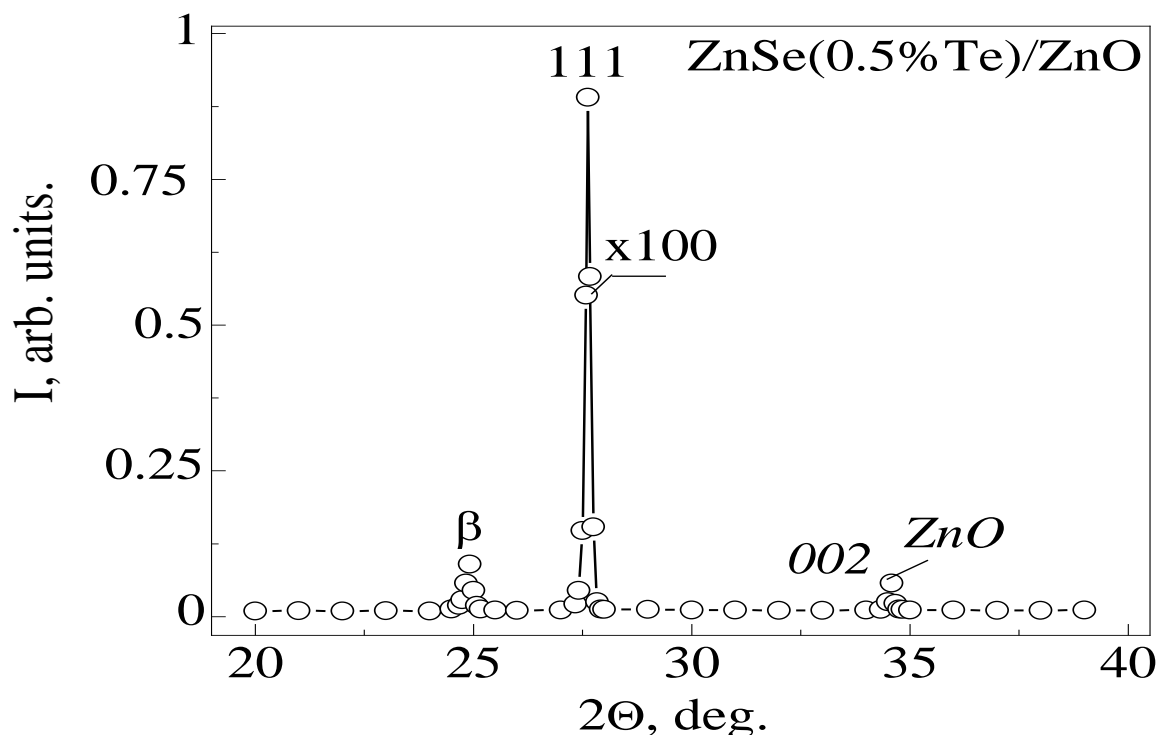
The figure shows the results of X-ray phase analysis (XPA) of ZnSe:O crystals before and after doping with an isovalent Te impurity [10, 17].



X-ray phase analysis of ZnSe:O.

The real intensity (311) is 100 times greater.

The ZnSe:O crystals were cut parallel to the close-packed (111) plane; accordingly, the most intense basic reflection (311) is visible on the X-ray pattern (Fig. 1). It can be seen that in the untreated ZnSe cubic crystal, low-symmetry ZnO impurity phase (103 reflection) and a very monotonic background are detected. This indicates that the ZnSe matrix lattice has relaxed and is no longer strained. Intensity ratio $I(103)/I(311) \sim 0.0091$. It follows from this that the initial ZnSe:O crystal apparently represents a structure in the surface layer of which ZnO NC were formed. The size of inclusions of the ZnO crystalline phase, determined by the Selyakov–Scherrer formula, was ~ 27 nm. It was shown in [5] that ZnSe crystals obtained by the Bridgman-Stockbarger method contained Te impurity from 0.5 to 3 wt.%, determined by the X-ray fluorescence method. Te isovalent impurity has positive effect on the structural perfection of ZnSe crystals. In the $\text{ZnSe}_{1-x}\text{Te}_x$ crystal at $C_{\text{Te}} < 0.3\text{wt.}\%$ twins and stacking faults were found, $C_{\text{Te}} \geq 0.6\text{wt.}\%$ leads to tetragonal distortion of the crystal lattice.



2. X-ray phase analysis of ZnSe(0,5wt%Te).

The real intensity (111) is 100 times greater.

As shown in fig. 2. ZnSe(0.5%Te)/ZnO nanoheterostructure (nonstoichiometry ratio was Se/Zn 0.853), grown in reducing medium, with crystallographic orientation (111), in the diffraction pattern, in addition to the main structural reflection (111) with $d/n=0.3271$ nm; on both sides of it are clearly distinguished above the background level along one diffraction line with low intensity. The analysis showed that one of them at $2\theta \sim 250$ is the β -component of the main selective reflection (111). On the other hand, the diffraction peak (103) at about $2\theta \sim 480$ belongs to the ZnO nanocrystalline phase up to 52 nm in size. Also, X-ray diffraction analysis showed that, depending on the composition and orientation of the crystals, the ZnSe matrix lattice gave reflections (111) and (311) in the region $2\theta=26 \sim 560$, and ZnO NC gave reflections (002) and (103) at $34 \sim 640$. In our case, the critical size of ZnO NP in ZnSe(Te) varied from 27 to 52 nm depending on the orientation of the substrate and the tellurium content. Thus, our results on XRD are consistent with the data of works published later [3, 6, 7].

Conclusions: The dependence of the critical dimensions, shape and orientation of ZnO nanocrystals on the corresponding orientation of the ZnSe crystal-substrate, due to the

minimization of lattice stresses at the interfaces of nanoheterostructures: 27 nm (103)ZnO/(311)ZnSe:O and 50 nm (002)ZnO/(111) ZnSe(0.5% Te);

REFERENCES

1. Красильник З.Ф. Наноструктуры для нанофотоники // Известия АН, серия физическая. – Москва. 2003. - Т.67, №2. – С.152-158.
2. Kripal R., Gupta A.K., Srivastava R.K., Mishra Sh.O. Journal of Spectrochimica Acta, Part A: Molecular and Biomolecular Spectroscopy – Elsevier. 79 (2011), P.1605-1612.
3. Лянгузов Н.В., Кайдашев В.Е., Кайдашев Е.М., Абдулвахидов К.Г. Письма в ЖТФ. - Санкт Петербург, 2011. – Т.37, №5. - С.1-8.
4. Лисицкий О.Л., Кумеков М.Е., Кумеков С.Е., Теруков Е.И. Физика и техника полупроводников. - Санкт Петербург, 2009. – Т.43, №6. – С.794-796.
5. Атрощенко Л.В., Воронкин Е.Ф., Галкин С.Н., Лалаянц А.И., Рыбалка Т.А., Рыжиков В.Д., Федоров А.Г. Неорганические материалы. - Москва, 2004. - Т.40, №6. - С.656-659.
6. Станчик А.В., Гременок В.Ф., Башкиров С.А., Тиванов М.С., Юшкенас Р.Л., Новиков Г.Ф., Герайтис Р., Саад А.М. Физика техника полупроводников. - Санкт Петербург, 2018. - Т.52, №2. - С.227-232.
7. Елюхина О.В., Соколовский Г.С., Кучинский В.И. Физика и техника полупроводников. - Санкт Петербург, 2007. – Т.41, №2. – С.129-133.
8. Elmurotova D.B., Ibragimova E.M. Semiconductors. - St. Petersburg, 2007. № 10 (41). - P.1135-1139.
9. Эльмуротова Д.Б., Каланов М.У., Ибрагимова Э.М., Вахидов Ш.А. Доклады Академии наук РУз. – Ташкент, 2008. № 2. С. 28–31.
10. Elmurotova D.B., Ibragimova E.M. Kalanov M. U., Tursunov N. A. Physics of the Solids State. - St. Petersburg, 2009. № 3 (51). P.456-464.
11. Elmurotova D.B., Ibragimova E.M. Technical Physics Letters. - St. Petersburg, 2010. № 6(36). P. 517-520.
12. Эльмуротова Д.Б., Ибрагимова Э.М. Физическая электроника UzPEC-5: Рес. конф. 28–30 октября, 2009. – Ташкент, 2009. – С. 182.

13. Elmurotova D.B., Ibragimova E.M., Kalanov M.U., Rustamova V.M. Current Problems in Nuclear Physics and Atomic Energy. 3th Int. Conf. June 7-12, 2010. - Keiv, 2010. - P. 136.
14. Elmurotova D.B., Ibragimova E.M., Kalanov M.U. Nanoscience Problems and prospects quantum function materials and devices, 9th Joint Uzbek-Korea Symposium November 2-5, 2010. – Ташкент, 2010. - С. 25.
15. Эльмуротова Д.Б., Ибрагимова Э.М. Физика и физическое образование: достижения и перспективы развития: 3 Межд. науч. конф. 19–25 августа 2011. – Бишкек, 2011. – С. 31-32.
16. Ibragimova E.M., Kalanov M.U., Mussaeva M.A., Elmurotova D.B., Rustamova V.M. Recent Advances in the Physics of Low-Dimensional Nanoscale Systems: Int. Workshop 10-11.11.2011. – Tashkent, 2011.-P.71-80.
17. Эльмуротова Д.Б., Ибрагимова Э.М. Современные проблемы физики полупроводников СПФП-2011. Мат. Рес. конф., 23–28 ноября 2011. – Нукус, 2011. – С. 117–119.
18. Эльмуротова Д.Б., Ибрагимова Э.М. Нанотехнология ва кайта тикланадиган энергия манбалари: муаммолар ва ечимлар: Рес. илмий-амалий конф. мат. 27-28 апрель, 2012. – Карши, 2012. – С. 206–208.
19. Elmurotova D.B., Ibragimova E.M. Dubna-nano 2012, Application of nanosystems, Int. Conf. July 9-14, 2012. - Dubna, Russia, 2012. - P. 12.
20. Elmurotova D.B, Mussaeva M.A., Ismatova L.N, Xaitov F.N. International Meeting and Conferences Research Association IMCRA Publication, Science, Education and innovations in the context of problems, 05 nov, 2021 Baku, International conference P.167-177 pp.